

PURE CO₂-OIL SYSTEM MINIMUM MISCIBILITY PRESSURE PREDICTION USING OPTIMIZED ARTIFICIAL NEURAL NETWORK BY DIFFERENTIAL EVOLUTION

Menad Nait Amar, Nourddine Zeraibi and Kheireddine Redouane

Department of Mining and Petroleum Engineering, Faculty of Hydrocarbons and Chemistry, University M'hamed Bougara- Boumerdes, 35000 Algeria

Received December 15, 2017; Accepted March 19, 2018

Abstract

Miscible CO₂ flooding is one of the most attractive enhanced oil recovery options thanks to its microscopic efficiency improvement. A successful implementation of this method depends mainly on the accurate estimation of minimum miscibility pressure (MMP) of the CO₂-oil system. As the determination of MMP through experimental tests (slim tube, and rising bubble apparatus (RBA)) is very expensive and time consuming, many correlations have been developed. However, all these correlations are based on limited set of experimental data and specified range of conditions, thus making their accuracies questionable. In this research, we propose to build robust, fast and cheap approach to predict MMP for pure CO₂-oil by applying hybridization of artificial neural networks with differential evolution (DE). DE is used to find best initial weights and biases of neural network. Four parameters that affecting the MMP are chosen as input variables: reservoir temperature, mole fraction of volatile-oil components, mole fraction of intermediate-oil components and molecular weight of components C5+. 105 MMP data covering wide range of conditions are considered from the published literature to establish the model. The obtained results demonstrate that our approach outperforms all the published correlations in term of accuracy and reliability.

Keywords: Pure CO₂ minimum miscibility pressure; carbon dioxide injection, artificial neural networks, differential evolution.

1. Introduction

With the technological advancement worldwide, demand for energy (mainly fuel energy) is growing exponentially thus requiring the creation of effective methods for tertiary recovery of the residual oil before the stage of reservoirs abandonment. Miscible gas injection, especially miscible CO₂ flooding, is one of well-established enhance oil recovery methods (EOR) during recent decades. This method is able to improve recovery of original oil in place over of 20% [1]. The right parametric design of miscible CO₂ injection depends greatly on a key factor: minimum miscible pressure (MMP), which is defined as the lowest pressure at which the flood changes from immiscible (multiple phase flow) to miscible (single phase flow) [2-4]. Hence an accurate estimation of MMP seems to be necessary.

MMP can be estimated using experimental tests such as slim tube [5], rising bubble apparatus (RBA) [6], multi-contact mixing-cell experiment [4] or the vanishing interfacial tension (VIT) technique [7]. Although the accuracy of these tests, all of them are very expensive and time consuming. An alternative way which is practicable on the slightest costs to calculate the MMP of CO₂-oil systems is insured by the available empirical/analytical correlations. However, as all these correlations have been developed under experimental data of CO₂-oil systems, they have certain constraints and conditions of application. Holm and Josendal first graphical MMP correlation for pure CO₂-oil [8] has been developed using crude oils with molecular weight of C5+ elements (MW_{C5+}) ranged between 180 g/mol and 240 g/mol, their experiment temperatures were between 32.2 °C and 82.5°C, and ranges of the MMP were between 9.65 MPa

and 22 MPa. Cronquist correlation [9] has been established with tested oil gravity ranged from 23.7 to 44.8°API, temperature ranged from 21.67 to 120.8°C and experimental MMP ranged from 7.4 to 34.5 MPa. Yellig & Metcalfe correlation [10] and Orr & Jensen correlation [11] were only suitable for reservoir temperatures of ($35^{\circ}\text{C} \leq T_R \leq 88.9^{\circ}\text{C}$) and ($T_R < 49^{\circ}\text{C}$) respectively. Emera-Sarma correlation [12] was limited to $40.8^{\circ}\text{C} < T_R < 112.2^{\circ}\text{C}$, $8.28 < \text{MMP} < 30.2\text{MPa}$ and $166.2 \text{ g/mol} < MW_{\text{C}5+} < 267.5 \text{ g/mol}$. Shokir correlation [13] was elaborated under $32.2^{\circ}\text{C} < T_R < 112.2^{\circ}\text{C}$, $6.9 < \text{MMP} < 30.28 \text{ MPa}$ and $185 \text{ g/mol} < MW_{\text{C}5+} < 268 \text{ g/mol}$. Other correlations such as Alston *et al.* [14], Orr and Silva [15], Glaso's [16], Lee [17], and Yuan *et al.* [18] have focused directly to a specific oil reservoirs, and this, cannot satisfy the level of comprehensiveness and generalization required by various other oil reservoirs where the characteristics are different.

Recently, Artificial Intelligence (AI) has been widely applied in the petroleum field to solve many conventional and unconventional problems [19-21]. Among AI methods, artificial neural networks (ANNs) is the famous one thanks to its effectiveness. ANNs create models that can recognize highly complex and non-straight-forward problems. As the miscibility concept is a high complex problem and as ANN is a robust tool in mapping input to output of complex relationship, this technique provides an integrated way for predicting CO₂ MMP.

ANN models can present some obvious defects and inaccuracies caused by the defaulted training algorithms (like backpropagation BP) that trap in local minima. Hence, in this paper, we propose to optimize the weights and thresholds of the neural networks with differential evolution algorithm (DE) (which belongs to global meta heuristic optimization algorithms) to comprehensively predict MMP in pure CO₂-oil systems. On other words, this approach consists in building a hybrid ANN-DE-BP with minimum error function. Four parameters are considered as the influence factors (inputs) of MMP pure CO₂-oil systems: the mole percentage of volatiles x_{vol} (includes C1 and N2), the mole percentage of intermediates x_{int} (contains C2-C4, CO₂ and H₂S), the molecular weight of C5+ oil components (MW_{C5+}) and reservoir temperature (T_R). The model is developed and tested using 105 data collected from published literature and covering a wide range of variables. The accuracy of the ANN-DE-BP model is compared with MMP values calculated from the ANN-BP (artificial neural network with defaulted back propagation learning) and some well-known correlations. In additions, several statistical indexes and graphical error analysis are performed to better judge the robustness and the reliability of ANN-DE-BP to predict MMP of pure CO₂-oil system.

2. Artificial Neural Network (ANN)

In order to find relationship between the input and output data derived from experimental works, a more powerful method than the traditional ones are necessary. Artificial Neural Network (ANN) is an especially efficient algorithm to approximate any function with finite number of discontinuities by learning the relationships between input and output vectors. ANN is a mathematical model inspired by the biological neural networks. It is a non-linear mapping model and has been successfully applied in many domains [19,22].

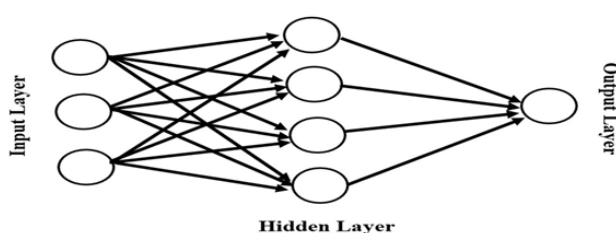


Fig. 1. An example of an ANN structure

It consists of many calculating units called nodes, these nodes are inside the layers: input data enter the first layer and output data exit the last layer. The layers between input and output layers are called hidden layers. For modeling purposes, the commonly used feed-forward ANN architecture namely multi-layer perceptron (MLP) may be employed. MLP involves an input layer, an output layer, and one (or more) hidden layer (s) with different roles. Each connecting line has an associated weight. Fig. 1 shows an example of typical 3-layer MLP.

The output from a given neuron is calculated by applying a transfer function to a weighted summation of its input to give an output, which can serve as input to other neurons, as follows [19]:

$$a_{jk} = g_k(\sum_{i=1}^{N_{k-1}} w_{ijk} a_{i(k-1)} + b_{jk}) \quad (1)$$

where a_{jk} are jth neuron outputs from kth layer and b_{jk} is the bias weight for neuron j in layer k. The model fitting parameters w_{ijk} are the connection weights. The nonlinear activation transfer functions g_k may have many different forms. The classical ones are threshold, sigmoid, Gaussian and linear function [23].

MLP training procedure aims at obtaining suitable weight set w_{ijk} and biases that minimizes a pre-specified error function such average absolute relative deviation percent (AARD %). The back propagation learning algorithm is the most commonly used algorithm. Several back-propagations training methodologies exist, which include the quasi-Newton backpropagation (BFGS), the Powell -Beale conjugate gradient, the Levenberge-Marguardt Algorithm (LMA) and others [19]. During the training, both the inputs and the outputs are provided. The network then processes the inputs and compares its resulting outputs against the desired outputs. Errors are then propagated back through the system, causing the system to adjust the weights which control the network. This process occurs over and over as the weights are continually tweaked.

According to [24-25], the convergence of the BP algorithm is highly dependent on the initial values of weights and biases. In the literature, using novel heuristic optimization methods or evolutionary algorithms is a popular solution to enhance the problems of BP-based learning algorithms.

3. Differential Evolution (DE)

Differential Evolution (DE) is a stochastic, population-based optimization algorithm introduced by Storn and Price in 1996 [26-27]. It is also one of the evolutionary algorithms. DE uses the similar genetic algorithm operators: crossover, mutation and selection. The main difference in constructing better solutions is that genetic algorithms rely on crossover while DE uses mutation operation as a search mechanism and selection operation to direct the search toward the prospective regions in the search space. The main steps of this algorithm are summarized as follows:

- *Initialization:* An optimization task consisting of D parameters can be represented by a D-dimensional vector. In DE, a population of NP solution vectors is randomly created at the start.
- *Mutation:* For each individual i of a generation G: $x_{i,G}$, a mutant vector is produced by:

$$v_{i,G+1} = x_{r1,G} + F * (x_{r2,G} - x_{r3,G}) \quad (2)$$

where $i, r1, r2, r3 \in \{1, 2, \dots, NP\}$: Population size} are randomly chosen and must be different from each other. F is called the mutation factor: it is a random number from [0,2]; and $v_{i,G+1}$ is called donor vector.

- *Recombination (crossover):* The parent vector is mixed with the mutated (donor) vector to produce a trial vector $u_{ji,G+1}$

$$u_{ji,G+1} = \begin{cases} v_{i,G+1}, & \text{if } (\text{rand}_{ij} \leq CR) \text{ or } j = I_{rand} \\ x_{ji,G}, & \text{if } (\text{rand}_{ij} > CR) \text{ and } j \neq I_{rand} \end{cases} \quad (3)$$

where $j = 1, 2, \dots, D$; $\text{rand}_{ij} \in [0, 1]$ is the random number; CR is crossover constant $\in [0, 1]$ and $I_{rand} \in (1, 2, \dots, D)$ is a randomly chosen index.

- *Selection:* The child produced after the mutation and crossover operations is evaluated. Then, the performance of the child vector and its parent is compared and the better one is selected. If the parent is still better, it is retained in the population.

$$x_{i,G+1} = \begin{cases} u_{i,G+1}, & \text{if } f(u_{i,G+1}) \leq f(x_{i,G}) \\ x_{i,G}, & \text{otherwise} \end{cases} \quad (4)$$

where f is the fitness function (the case shown in the equation 4 corresponds to minimize the fitness function).

The implementation of the differential evolution algorithm to optimize the weights and biases of ANN is illustrated in Fig. 2.

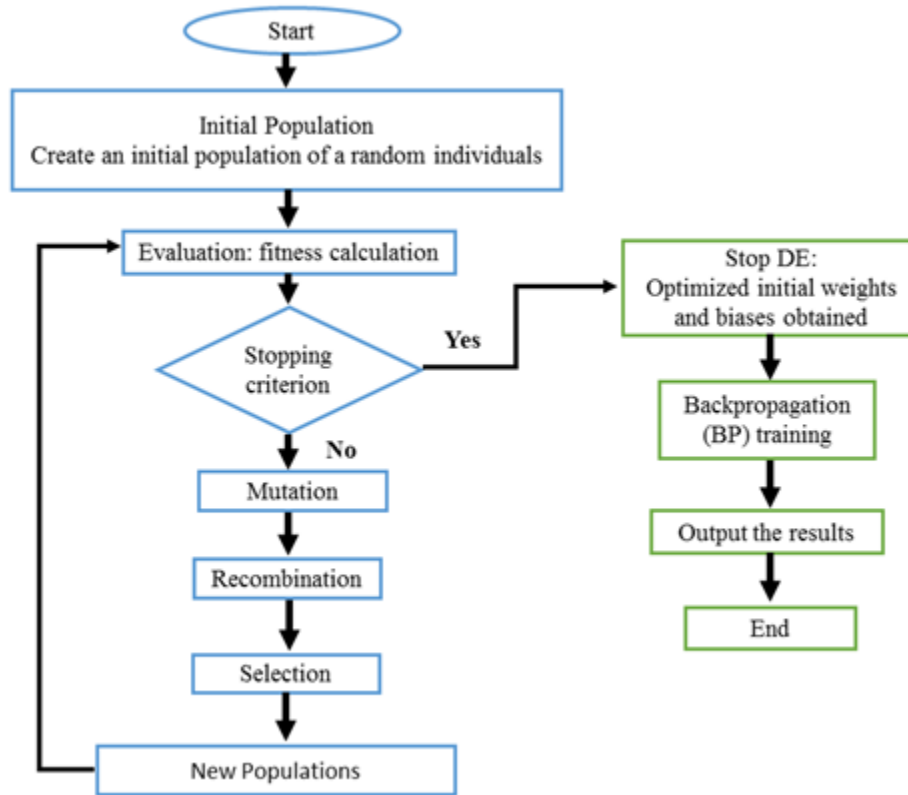


Fig. 2. Implementation of DE to MMP ANN's training

4. Data analysis

105 data sets are collected from published literature [9-18, 28-34] with a wide range of temperatures and oil compositions. Reservoir temperature for this dataset ranged from 34.4 to 137.2°C, while the molecular weight of the C5+ fraction varied from 136.26 to 391 g/mol. Table 1 shows a full statistical description of the collected and used data in the development of the model.

Table 1. Ranges and their corresponding statistical parameters of the input/output data used for developing the model

	Variables	Max	Min	Mean	SD
Inputs	Output MMP (MPa)	38.5	7.93	17.40	6.99
	MW _{C5+} (g/mol)	391	136.26	205.43	39.65
	T _R (°C)	137.22	34.4	74.38	26.11
	x _{vol} (%)	54.3	0	20.43	15.65
	x _{int} (%)	43.5	0	18.77	12.33

To demonstrate the correlation between MMP and the used independent variables, the correlation matrix is implemented [35]. This matrix illustrates the power of a linear relationship between two different variables in multi-variables system [35]. The coefficient between two variables x and y, is defined by the following formula:

$$r_{xy} = \frac{\sigma_{xy}}{\sigma_x \sigma_y} \quad (5)$$

where σ_x and σ_y are the sample standard deviations, and σ_{xy} is the sample covariance.

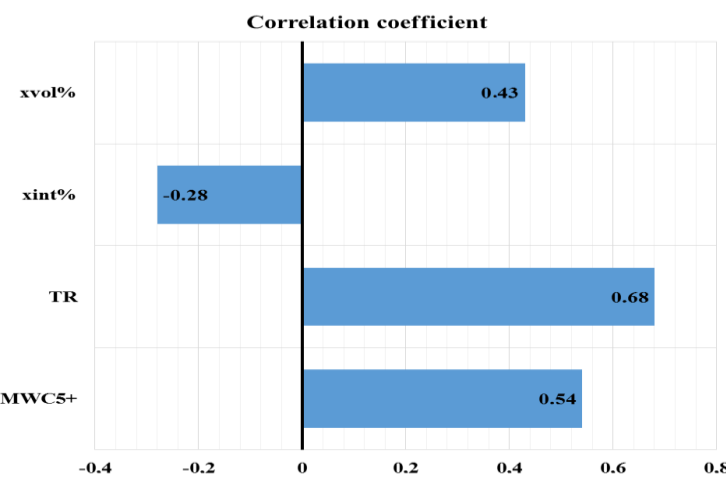


Fig. 3. Correlation coefficient of the independent variables

fraction of the intermediate elements (x_{int}) has a negative linearly relation with MMP which means that MMP is high, if x_{int} is low.

5. Model development

To improve the convergence conditions during the development of the model, the used data are normalized at the interval [-1 1] according to the following equation:

$$x_{normalized} = \frac{2(x_i - x_{min})}{(x_{max} - x_{min})} - 1 \quad (6)$$

where $x_{normalized}$ is the normalized value of x_i , x_{max} and x_{min} are the maximum and minimum values of the variable x respectively (as shown in Table 1).

The first step to establish an ANN-DE-BP model to estimate MMP of pure CO₂-oil systems consists in achieving to a best ANN topology. One hidden layer is employed in our study, as it is proven in the literature [36] that a MLP network having only one hidden layer can estimate most of nonlinear systems. The number of neurons in the hidden layer is established using trial and error method: after a series of optimization processes by monitoring the performance of the network until the best network structure is accomplished. The radial basis activation function is used as the transfer function from input layer to hidden layer, and the linear function is taken as the activation function in the last layer. Then the problem is formulated as an optimization problem to find a set of weights and biases of the ANNs that minimizes the difference between the predictions and the target values in the training set of data using differential evolution algorithm (by following flowchart of Fig. 2). 88 points of the 105 are selected randomly and employed in the training process while the remain 17 are used to test the model. The features of implemented algorithm are summarized as follows: population size: 50, max number of generation: 100 and crossover's constant: 0.8. All the programming tasks developed in this work are carried out using MATLAB® 2016-a computing environment [37].

To evaluate the developed model and its predictive performances, it must be compared against existing correlations and approaches. This is done through cross plots and a group error analysis, using the average absolute percent error (AAARD%), standard deviation (SD), the correlation factor (R^2) and the root mean square error (RMSE). These statistical indexes can be mathematically expressed by the following equations:

$$AAARD\% = \frac{1}{N} \sum_{i=1}^N \left| \frac{MMP_i^{exp} - MMP_i^{cal}}{MMP_i^{exp}} \right| \times 100 \quad (7)$$

Its values are between [-1 1]. Two variables are said to be positively linearly related if their correlation coefficient is close to 1 and negatively linearly if it is close to -1. For values nearby zero, it would indicate a weak linear relationship between the variables. The obtained results are shown in Fig. 3.

The graph certifies that reservoir temperature (T_R) has the highest linearly relation with MMP (0.68). Then Molecular Weight (MW) of the C5 + and x_{vol}% by 0.54 and 0.43, respectively. Furthermore, it can be deduced that molar

$$SD = \sqrt{1/(N-1) \sum_{i=1}^N \left(\frac{MMP_i^{exp} - MMP_i^{cal}}{\overline{MMP}^{exp}} \right)^2} \quad (8)$$

$$R^2 = 1 - \frac{\sum_{i=1}^N (MMP_i^{exp} - MMP_i^{cal})^2}{\sum_{i=1}^N (MMP_i^{cal} - \overline{MMP})^2} \quad (9)$$

$$RMSE = \sqrt{\frac{1}{N} \sum_{i=1}^N (MMP_i^{exp} - MMP_i^{cal})^2} \quad (10)$$

where N represents the number of the measured information, MMP_i^{exp} is the experimental minimum miscibility pressure values, while MMP_i^{cal} is the calculated MMP values which are predicted by the developed model. Average value of the MMP data is shown by \overline{MMP} .

6. Results and discussion

Table 2 shows the results of performed sensitivity analysis for investigation of the number of neurons in the hidden layer for ANN-BP. In this table, only topologies which have been trained several times and show a high degree of accuracy are presented. The optimal configuration has been selected by finding the structure which has a high accuracy based on the statistical error analysis. It can be clearly seen that 16 is the best number of neurons in the hidden layer, and the configuration $4 \times 16 \times 1$ (one input layer containing the inputs showed in Table 1, one hidden layer with 16 nodes and one output layer containing one node which is MMP) can be considered as an optimal topology in this study.

Table 2. Sensitivity analysis for various ANN topologies (training data)

Number of hidden neurons	AARE (%)	R ²	SD	RMSE
9	8.46	0.9607	0.11	1.87
10	6.91	0.9743	0.097	1.82
12	6.99	0.9719	0.093	1.89
15	7.52	0.9604	0.11	1.88
16	6.16	0.9681	0.085	1.72
19	6.37	0.970	0.089	1.74

Cross plots between output and target values for training and test data of ANN-DE-BP and ANN-BP models are illustrated in Fig. 4. For each model, all the predicted values are sketched against the experimental values, and therefore across plot is created and compared against a unit slope line that shows the perfect model line: the closer the plotted data to this line, the higher is the reliability of the model. According to these cross plots, ANN-DE-BP model has closer match to the real values. For a deep comparison, Table 3 presents the results of performance evaluation through the aforementioned statistical indicators. According to this table, ANN-DE-BP has a reliable ability to predict MMP with a total AARD% of 5.92%, RMSE of 1.47, high correlation coefficient ($R^2=0.9808$) and low standard deviation ($SD=0.0817$). Furthermore, this table depicts that ANN-DE-BP outperforms largely ANN-BP model.

Table 3. Performance analysis of ANN-BP and ANN-DE-BP

	R ²	AARD (%)	RMSE	SD
ANN-BP	Training (88 data)	0.9681	6.16	1.72
	Test (17 data)	0.9491	13.88	3.26
	All (105 data)	0.9650	7.41	1.97
ANN-DE-BP	Training (88 data)	0.9807	5.17	1.33
	Test (17 data)	0.9811	9.81	2.23
	All (105 data)	0.9808	5.92	1.47

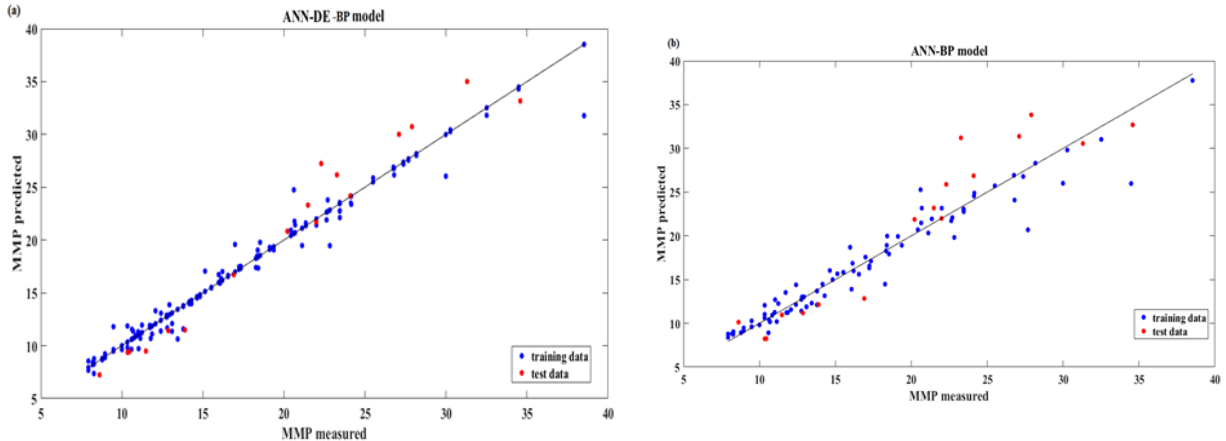


Fig. 4. Cross-Plots of the Results: (a) MMP measured vs MMP ANN-DE-BP (training + test); (b) MMP measured vs MMP ANN-BP (training + test)

To find better comprehension on the performance of the model, cumulative distribution function (CDF) plot of the predicted errors is shown in Fig. 5. In this figure, the error is the percent relative error (PRE%) which measures the relative deviation of predicted data from the experimental data. Also, details of this figure are presented in Table 4 using concept of the probability distributions of the errors. Table 4 and Fig. 5 reveal that 80 % of the ANN-DE-BP prediction values have an absolute error less than 10%, and only 3% with an absolute error up to 20%.

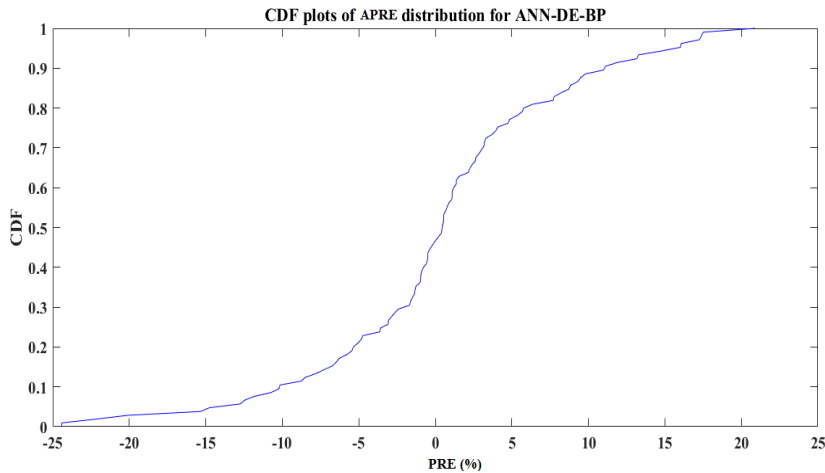


Fig. 5. CDF plot of APRE of ANN-DE-BP

Table 4. Probability distribution of the simple errors for used data

Error	ANN-DE-BP	Error	ANN-DE-BP
$ APRE < 0.16$	0.019	$ APRE < 7.80$	0.70
$ APRE < 0.53$	0.10	$ APRE < 10.00$	0.80
$ APRE < 1.00$	0.21	$ APRE < 14.75$	0.90
$ APRE < 1.50$	0.30	$ APRE < 17.38$	0.95
$ APRE < 2.65$	0.40	$ APRE < 20.00$	0.97
$ APRE < 3.70$	0.50	$ APRE < 24.40$	1
$ APRE < 5.45$	0.60		

To investigate and to provide more insight into the validity of the proposed model for MMP estimation in pure CO₂-oil systems, seven of well-known correlations have been selected for comparison. Table 5 shows the results. It can be seen from the analysis of comparison that

ANN-DE-BP proves its ability in MMP prediction of the pure CO₂-oil systems with high precision and lowest average absolute deviation among all correlations and ANN with backpropagation learning.

Table 5. Comparison of ANN-DE-BP performances against existing correlations

Model / correlation	R ²	AARD (%)	RMSE	SD	Max AARD (%)
ANN-DE-BP	0.9808	5.92	1.47	0.0817	24.40
ANN-BP	0.9650	7.41	1.97	0.098	34.10
Cronquist	0.9043	16.42	4.23	0.2085	69.13
Lee	0.6393	19.73	6.05	0.2782	98.68
Yelling Metcalfe	0.6771	18.01	6.06	0.2341	66.09
Orr-Jensen	0.6331	20.17	6.71	0.2548	78.71
Alston et al.	0.8546	19.15	6.05	0.2640	91.54
Emara-Sarma	0.8868	14.02	3.92	0.1867	56.82
Shokir	0.8574	12.58	3.45	0.1674	57.94

Finally, for utilizing of our best-established model (i.e. ANN-DE-BP) and exact reproducing its results, the detailed information (its weight and bias matrixes) are reported in Table 6. This model contains one input layer (containing the inputs as arranged in Table 1), one hidden layer (it contains 16 nodes) and one output layer (contains one node) which is MMP. The radial basis activation function is used as the transfer function from input layer to hidden layer, and the linear function is taken as the activation function in the last layer. The normalization of dataset followed is expressed in equation (6) with respect to the bounds shown in Table 1.

Table 6. Weights and biases of the ANN-DE-BP

Neurons	Weight values of connections between input and hidden layer				
1	-2.6435	-2.8768	-0.4822	0.3454	
2	-2.4828	-0.6234	-0.8255	0.3686	
3	0.1751	-0.6750	3.6811	-0.6295	
4	2.3005	-2.4885	-1.1044	-1.3275	
5	0.3134	0.6956	-3.1345	0.9178	
6	-2.6354	-0.1521	1.5074	-2.2200	
7	0.0636	-0.2535	0.3671	-1.0719	
8	-2.4234	-0.3067	-0.6915	1.0496	
9	3.9934	-2.9587	-0.1020	0.9007	
10	2.5631	-2.6922	-0.8403	-0.4032	
11	0.2141	0.3385	-0.8303	-1.1127	
12	3.3936	3.5477	0.2842	0.3107	
13	-1.0396	1.0211	-0.1439	-2.7147	
14	4.1151	2.8660	0.5029	1.7354	
15	1.4882	-1.8420	-3.7362	-1.2947	
16	2.1720	0.9226	1.8268	0.0507	

Weight values of connections between hidden and output layer															
-0.5965	0.3559	1.1612	-0.3095	-1.5506	-0.3876	2.9475	-0.9274	0.0064	1.2707	3.9655	2.4085	-1.5664	-0.3002	-0.3924	-1.8314
Biases of the hidden layer															
-2.8664	3.4227	2.0303	-1.9878	-1.6632	0.7837	0.9189	-1.8503	2.1158	-0.7092	-1.5149	2.3326	2.5369	3.5869	0.3510	3.3695
Biases of the output layer															
-0.8889															

7. Conclusion

In this study, a new approach to predict MMP of pure CO₂-oil systems is proposed by optimizing artificial neural network with differential evolution (DE). This latter is used to optimize weights and biases of a pre-established neural networks. The results generated by this model i.e. ANN-DE-BP, are then compared with the experimental results, those generated by neural network with backpropagation learning and those generated by the existing approaches. The results show an excellent agreement between the model predictions and experimental data ($R^2 > 0.98$), and this model outperforms all other approaches. Furthermore, ANN-DE-BP provides a considerable improvement over previous proposed correlation with broader applicability in terms of accuracy and independent variable ranges.

List of symbols

MMP	minimum miscibility pressure (MPa)
MW_{C5+}	molecular weight of C5+ elements (g/mol)
X_{vol}	mole percentage of volatiles (includes C1 and N2)
X_{int}	mole percentage of intermediates (contains C2-C4, CO ₂ and H ₂ S)
T_R	reservoir temperature (°C)
ANN	artificial neural network
DE	differential evolution
BP	back propagation
$AARD$	average absolute percent error (%)
SD	standard deviation
R^2	the correlation factor
$RMSE$	root mean square error

References

- [1] Grigg RB, Schechter DS. State of the Industry in CO₂ Floods. in: SPE Annu. Tech. Conf. Exhib., Society of Petroleum Engineers, 1997. doi:10.2118/38849-MS.
- [2] Benmekki EH, Mansoori GA. Minimum miscibility pressure prediction with equations of state. SPE (Society Pet. Eng. Reserv. Eng.; (United States). 1988; 3:2.
- [3] Fazlali A, Nikookar M, Agha-Aminiha A, Mohammadi AH. Prediction of minimum miscibility pressure in oil reservoirs using a modified SAFT equation of state. Fuel, 2013; 108: 675–681.
- [4] Jaubert J-N, Wolff L, Neau E, Avaullee L. A Very Simple Multiple Mixing Cell Calculation To Compute the Minimum Miscibility Pressure Whatever the Displacement Mechanism. Ind. Eng. Chem. Res., 1998; 37: 4854–4859.
- [5] Wu RS, Batycky JP. Evaluation of Miscibility from Slim Tube Tests. J. Can. Pet. Technol., 1990; 29(6): doi.org/10.2118/90-06-06.
- [6] Christiansen RL, Haines HK. Rapid Measurement of Minimum Miscibility Pressure With the Rising-Bubble Apparatus, SPE Reserv. Eng., 1987; 2: 523–527.
- [7] Orr FM, Jessen K. An analysis of the vanishing interfacial tension technique for determination of minimum miscibility pressure, Fluid Phase Equilib., 2007; 255: 99–109.
- [8] Holm LW, Josendal VA. Mechanisms of Oil Displacement by Carbon Dioxide, J. Pet. Technol., 1974; 26:1427–1438.
- [9] Cronquist C. Carbon dioxide dynamic miscibility with light reservoir oils, in: Proc. 4th Annu. U.S. DOE Symp., 1978: pp. 28–30.
- [10] Yellig WF, Metcalfe RS. Determination and Prediction of CO₂ Minimum Miscibility Pressures (includes associated paper 8876, J. Pet. Technol., 1980; 32: 160–168.
- [11] Orr FM, Jensen CM. Interpretation of Pressure-Composition Phase Diagrams for CO₂/Crude-Oil Systems, Soc. Pet. Eng. J., 1984; 24: 485–497.
- [12] Emera MK, Sarma HK. Use of genetic algorithm to estimate CO₂-oil minimum miscibility pressure—a key parameter in design of CO₂ miscible flood, J. Pet. Sci. Eng., 2005; 46: 37–52.
- [13] Shokir EME-M. CO₂-oil minimum miscibility pressure model for impure and pure CO₂ streams, J. Pet. Sci. Eng., 2007; 58: 173–185.
- [14] RB Alston, GP Kokolis, CF. James, CO₂ Minimum Miscibility Pressure: A Correlation for Impure CO₂ Streams and Live Oil Systems, Soc. Pet. Eng. J., 1985; 25: 268–274.
- [15] Orr FM, Silva MK. Effect of Oil Composition on Minimum Miscibility Pressure-Part 2: Correlation, SPE Reserv. Eng., 1987; 2: 479–491.

- [16] Glaso O. Generalized Minimum Miscibility Pressure Correlation (includes associated papers 15845 and 16287), *Soc. Pet. Eng. J.*, 1985; 25: 927–934.
- [17] Lee JI. Effectiveness of carbon dioxide displacement under miscible and immiscible conditions, Rep. RR-40, Pet. Recover. Inst., Calgary. (1979).
- [18] Yuan H, Johns RT, Egwuenu AM, Dindoruk B. Improved MMP Correlation for CO₂ Floods Using Analytical Theory, *SPE Reserv. Eval. Eng.*, 2005; 8: 418–425.
- [19] Gharbi RBC., Mansoori GA. An introduction to artificial intelligence applications in petroleum exploration and production, *J. Pet. Sci. Eng.*, 2005; 49: 93–96.
- [20] Vaferi B, Eslamloueyan R, Ayatollahi S. Automatic recognition of oil reservoir models from well testing data by using multi-layer perceptron networks, *J. Pet. Sci. Eng.*, 2011; 77: 254–262.
- [21] Vafaei MT, Eslamloueyan R, Ayatollahi S. Simulation of steam distillation process using neural networks, *Chem. Eng. Res. Des.*, 2009; 87: 997–1002.
- [22] Hornik K, Stinchcombe M, White H. Multilayer feedforward networks are universal approximators, *Neural Networks*, 1989; 2: 359–366.
- [23] Bulsari AB. Neural networks for chemical engineers, Elsevier, 1995.
- [24] Zhang J-R, Zhang J, Lok T-M, Lyu MR. A hybrid particle swarm optimization-back-propagation algorithm for feedforward neural network training, *Appl. Math. Comput.*, 2007; 185: 1026–1037.
- [25] Mirjalili S, Mohd Hashim SZ, Sardroodi HM. Training feedforward neural networks using hybrid particle swarm optimization and gravitational search algorithm, *Appl. Math. Comput.*, 2012; 218: 11125–11137.
- [26] Storn R, Price K. Differential Evolution – A Simple and Efficient Heuristic for global Optimization over Continuous Spaces, *J. Glob. Optim.*, 1997; 11: 341–359.
- [27] Storn R. Differential evolution design of an IIR-filter, in: *IEEE Int. Conf. Evol. Comput.*, IEEE, 1996: 268–273.
- [28] H Zhang, D Hou, Li K. An improved CO₂-crude oil minimum miscibility pressure correlation, *J. Chem.*, 2015; 2015: Article ID 175940, <http://dx.doi.org/10.1155/2015/175940>
- [29] Adekunle O. Experimental approach to investigate minimum miscibility pressures in the Bakken, (2014).
- [30] Adyani WN, Kechut NI. Advanced Technology for Rapid Minimum Miscibility Pressure Determination (Part 1), in: *Asia Pacific Oil Gas Conf. Exhib.*, Society of Petroleum Engineers, 2007. doi:10.2118/110265-MS.
- [31] Dicharry RM, Perryman TL, Ronquille JD. Evaluation and Design of a CO₂ Miscible Flood Project-SACROC Unit, Kelly-Snyder Field, *J. Pet. Technol.*, 1973; 25: 1309–1318.
- [32] Dong M, Huang S, Dyer SB., Mourits FM. A comparison of CO₂ minimum miscibility pressure determinations for Weyburn crude oil, *J. Pet. Sci. Eng.*, 2001; 31: 13–22.
- [33] Elsharkawy AM, Poettmann FH, Christiansen RL. Measuring Minimum Miscibility Pressure: Slim-Tube or Rising-Bubble Method?, in: *SPE/DOE Enhanc. Oil Recover. Symp.*, Society of Petroleum Engineers, 1992. doi:10.2118/24114-MS.
- [34] Winzinger R, Brink JL, Patel KS, Davenport CB, Patel YR, Thakur GC. Design of a Major CO₂ Flood, North Ward Estes Field, Ward County, Texas, *SPE Reserv. Eng.*, 1991; 6: 11–16.
- [35] Vaferi B, Samimi F, Pakgohar E, Mowla D. Artificial neural network approach for prediction of thermal behavior of nanofluids flowing through circular tubes. *Powder Technol.*, 2014; 267: 1–10.
- [36] Cybenko G. Approximation by superpositions of a sigmoidal function. *Math. Control. Signals Syst.* 1992; 5: 455.
- [37] MATLAB®, MathWorks, Inc, 2016a, (n.d.).

To whom correspondence should be addressed: Menad Nait Amar, Faculty of Hydrocarbon and Chemistry University M'hamed Bougara- Avenue de l'indépendance, Boumerdes, 3500, Algeria, manad1753@gmail.com